Abnormal accumulation and recycling of glycoproteins visualized in Niemann–Pick type C cells using the chemical reporter strategy

Ngalle Eric Mbua[a,b], Heather Flanagan-Steet[b], Steven Johnson[b], Margreet A. Wolfert[b], Geert-Jan Boons[a,b,1], and Richard Steet[b,c,1]

[a]Department of Chemistry, [b]Complex Carbohydrate Research Center, and [c]Department of Biochemistry and Molecular Biology, University of Georgia, Athens, GA 30602

Edited* by Carolyn R. Bertozzi, University of California, Berkeley, CA, and approved May 6, 2013 (received for review December 4, 2012)

Niemann–Pick type C (NPC) disease is characterized by impaired cholesterol efflux from late endosomes and lysosomes and secondary accumulation of lipids. Although impaired trafficking of individual glycoproteins and glycolipids has been noted in NPC cells and other storage disorders, there is currently no effective way to monitor their localization and movement *en masse*. Using a chemical reporter strategy in combination with pharmacologic treatments, we demonstrate a disease-specific and previously unrecognized accumulation of a diverse set of glycoconjugates in NPC1-null and NPC2-deficient fibroblasts within endocytic compartments. These labeled vesicles do not colocalize with the cholesterol-laden compartments of NPC cells. Experiments using the endocytic uptake marker dextran show that the endosomal accumulation of sialylated molecules can be largely attributed to impaired recycling as opposed to altered fusion of vesicles. Treatment of either NPC1-null or NPC2-deficient cells with cyclodextrin was effective in reducing cholesterol storage as well as the endocytic accumulation of sialoglycoproteins, demonstrating a direct link between cholesterol storage and abnormal recycling. Our data further demonstrate that this accumulation is largely glycoproteins, given that inhibitors of *O*-glycan initiation or *N*-glycan processing led to a significant reduction in staining intensity. Taken together, our results provide a unique perspective on the trafficking defects in NPC cells, and highlight the utility of this methodology in analyzing cells with altered recycling and turnover of glycoproteins.

The fatal lysosomal disorder Niemann–Pick type C (NPC) results from mutations in genes encoding NPC1 or NPC2, proteins that act in coordination to mediate the efflux of unesterified cholesterol from lysosomes (1, 2). Loss of these proteins causes abnormal accumulation of cholesterol in neurons and other cell types, resulting in neuronal degeneration and hepatosplenomegaly (3–5). The pathophysiology of NPC disease is complex and incompletely understood. NPC-associated phenotypes may be related to the primary accumulation of cholesterol and secondary storage of other lipids, such as glycosphingolipids and sphingosine (6–9). Accompanying lipid storage, NPC cells exhibit defects in endocytic transport, such as altered recycling of specific cell surface glycoproteins, which also may be associated with diseases (10–14).

The molecules and pathways implicated in the latter defects have been difficult to analyze, owing to a lack of technology that can monitor the localization and accumulation of endogenous glycoproteins and glycolipids *en masse*. Although the analysis of single glycoprotein markers, such as the transferrin receptor, has provided some insight into NPC-associated trafficking defects, the use of individual glycoproteins limits the range of itinerant pathways that can be effectively probed and might not be representative of all cell surface molecules. In addition, trafficking studies have used the exogenous addition of tagged glycolipids, which may behave differently than their natural counterparts (15). Thus, the ability to track the endocytosis and intracellular trafficking of bulk glycoconjugates would be advantageous, providing a means to follow endogenously produced glycolipids and glycoproteins within NPC cells, overcoming the current limitations.

The chemical reporter strategy, pioneered by Bertozzi and coworkers (16–19), is emerging as a versatile approach to visualizing and capturing glycoconjugates of living systems. In this approach, a unique chemical functionality (reporter) is incorporated into glycoconjugates by feeding a modified biosynthetic precursor. The latter can then be reacted with a complementary bioorthogonal functional group, which in turn is linked to a probe. The azide is the most versatile chemical reporter because of its small size, bio-orthogonality, and diverse mode of reactivity. It can be tagged by Staudinger ligation using modified phosphines, by a copper (I)-catalyzed cycloaddition with terminal alkynes (CuAAC), or by a strain-promoted alkyne-azide cycloaddition (SPAAC) using cyclooctynes (20, 21). Such chemical reporter strategies can be used to monitor the trafficking of glycans within cells and to localize the expression of specific classes of glycans within living organisms, such as developing zebrafish embryos or *Caenorhabditis elegans* (21–25). Insights into the functional relevance of glycans in normal and disease biology have yet to emerge from these technologies, however. Here we demonstrate a previously unrecognized accumulation of glycoproteins in NPC1-null and NPC2-deficient fibroblasts using a powerful combination of SPAAC-based chemical reporter strategy and pharmacologic treatments. These studies provide insight into trafficking defects in NPC cells and highlight the utility of visualizing glycoconjugates *en masse* to uncover aspects of disease.

Results

Glycoconjugates Accumulate Intracellularly in NPC Fibroblasts. Control and disease fibroblasts were fed the sialic acid precursor peracetylated *N*-α-azidoacetylmannosamine (Ac_4ManNAz; Fig. 1*A*), which can be incorporated into glycoproteins and gangliosides as *N*-azidoacetyl sialic acid (SiaNAz). The resulting azido-modified glycoconjugates were visualized by confocal microscopy after cycloaddition with biotin-modified dibenzylcyclooctynol (DIBO; Fig. 1), followed by treatment with streptavidin-568. DIBO was chosen for this study because of its ability to detect both intracellular and extracellular glycoconjugates (21, 26). Although staining of Golgi, cell surface, and extracellular matrix was detected primarily in control fibroblasts, a striking additional accumulation of sialylated

Author contributions: N.E.M., H.F.-S., M.A.W., G.-J.B., and R.S. designed research; N.E.M., H.F.-S., S.J., M.A.W., G.-J.B., and R.S. performed research; G.-J.B. contributed new reagents/analytic tools; N.E.M., H.F.-S., S.J., M.A.W., G.-J.B., and R.S. analyzed data; and G.-J.B. and R.S. wrote the paper.

The authors declare no conflict of interest.

*This Direct Submission article had a prearranged editor.

[1]To whom correspondence may be addressed. E-mail: gjboons@ccrc.uga.edu or rsteet@ccrc.uga.edu.

This article contains supporting information online at www.pnas.org/lookup/suppl/doi:10.1073/pnas.1221105110/-/DCSupplemental.

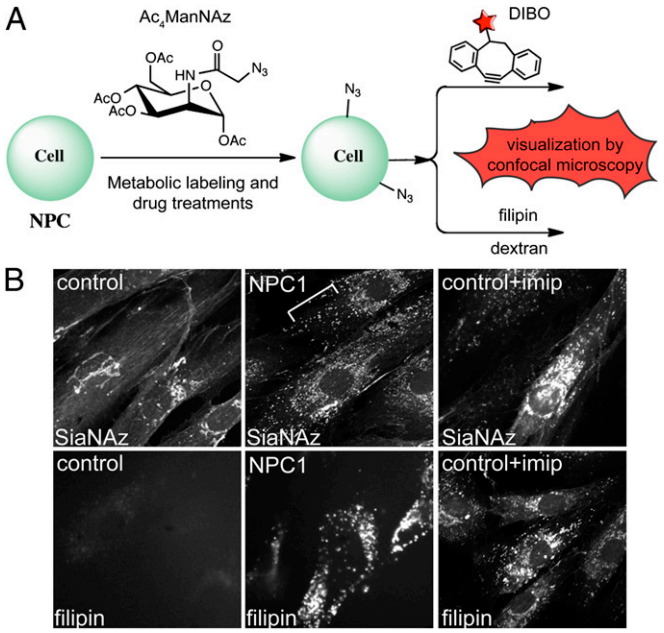

Fig. 1. Sialylated molecules accumulate within intracellular vesicles in NPC1-null fibroblasts and imipramine-treated control fibroblasts. (*A*) Bio-orthogonal chemical reporter strategy for monitoring glycoconjugate localization and trafficking in NPC cells. Cells fed with Ac_4ManNAz were subjected to SPAAC and visualized by confocal microscopy. Staining with filipin or antibodies to various marker proteins was used to colocalize sialylated molecules with cholesterol or compartment-specific proteins. Several pharmacologic compounds were used to determine the nature of labeled molecules and to alleviate the cholesterol storage associated with NPC disease. (*B*) (*Upper*) Ac_4ManNAz-labeled control, NPC1-null fibroblasts, and imipramine (imip)-treated control fibroblasts incubated with DIBO and streptavidin-conjugated fluorophore. (*Lower*) Filipin staining of the same cells under the same conditions. Imipramine treatment of control fibroblasts led to a similar accumulation of sialylated glycoconjugates as seen in NPC fibroblasts. n = 26–30 cells scored per condition; four independent experiments. The phenotype was present in >95% of cells.

glycoconjugates was observed within intracellular vesicles in NPC1-null (Fig. 1*B*) and NPC2-deficient (Fig. S1) fibroblasts. This phenotype appeared to be specific to NPC cells, given that no obvious vesicular accumulation was noted in mucolipidosis IV (ML-IV) or mucopolysaccharidosis I (MPS-I) fibroblasts (Fig. S1), which exhibit different types of storage defects. Furthermore, treatment of control fibroblasts with the antidepressant imipramine, a known chemical inducer of intracellular cholesterol storage (27), also resulted in the accumulation of sialylated glycoconjugates (Fig. 1*B*), whereas treatment with the antidepressant phenelzine did not induce cholesterol storage or cause this type of phenotype (Fig. S1). These observations suggest a correlation between cholesterol and glycoconjugate buildup within intracellular vesicles.

To further probe the specificity of the storage, we labeled cells with peracetylated *N*-α-azidoacetylgalactosamine (Ac_4GalNAz), which can be incorporated into *O*-linked glycans, glycosaminoglycans and glycolipids. In this case, azido-modified glycoconjugates in control cells were detected primarily within the nucleus, extracellular matrix, and Golgi bodies, whereas NPC1-null fibroblasts again exhibited additional vesicular staining (Fig. S2). The GalNAz phenotype was also seen in NPC2-deficient fibroblasts and imipramine-treated control cells, although the intensity of staining was somewhat reduced compared with SiaNAz. Taken together, these data indicate that storage of cholesterol, induced by genetic or chemical means, is associated with the intracellular accumulation of a wide variety of glycoconjugates.

Glycoconjugates Are Excluded from Cholesterol-Laden Compartments. To examine possible colocalization of the accumulated glycoconjugates with cholesterol-filled lysosomes, we metabolically labeled NPC1-null cells with Ac_4ManNAz and visualized the resulting sialylated compounds by successive treatment with DIBO-biotin and streptavidin Alexa Fluor 568, with costaining with filipin to detect cholesterol. The resulting fluorescence images clearly demonstrated little or no colocalization of cholesterol- and SiaNAz-positive vesicles (Fig. 2*A*), indicating that internal cell surface sialoglycoconjugates are excluded from cholesterol-laden lysosomes of NPC cells. Complete separation of sialylated glycoconjugates and cholesterol was also seen in NPC2-deficient fibroblasts, further demonstrating that cholesterol storage, and not impaired NPC1 function, is the primary mechanism underlying the exclusion of SiaNAz-positive molecules from cholesterol-containing compartments (Fig. S3).

To better define the localization of the SiaNAz-positive vesicles in NPC1-null fibroblasts, we subjected Ac_4ManNAz-labeled control and NPC1-null fibroblasts to DIBO-biotin and incubated them with antibodies against early endosome antigen protein 1 (EEA1) for identification of early endosomes, CD63 for late endosomes and multivesicular bodies, and lysosomal-associated membrane protein 1 (LAMP1) for lysosomes. Partial colocalization of SiaNAz-positive vesicles with CD63, but not with EEA1 or LAMP1, was apparent in NPC1-null cells, suggesting that much of the NPC-dependent glycoconjugate storage occurs within endosomes (Fig. 2*B*). The lack of colocalization with LAMP1 was expected, because this marker exhibited a high degree of overlap with filipin-stained cholesterol in NPC1-null cells. In contrast, no significant colocalization with any of the markers was detected in control cells. We cannot rule out the possibility that CD63 is mislocalized in NPC1-null cells. Indeed, there was a marked increase of CD63 staining in NPC1-null cells, likely reflecting either a proliferation of endosomal

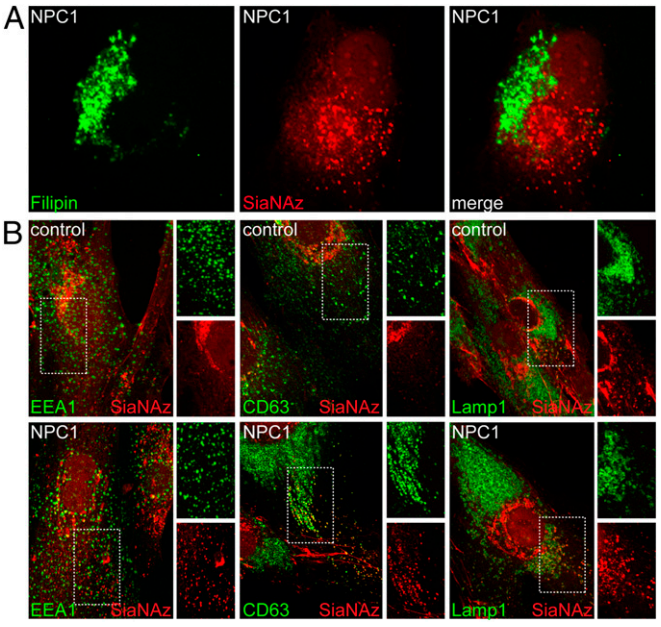

Fig. 2. SiaNAz-labeled molecules are excluded from cholesterol-laden compartments and exhibit partial colocalization with endosomal markers in NPC1-null fibroblasts. (*A*) NPC1-null fibroblasts were labeled with Ac_4ManNAz and incubated with DIBO and streptavidin Alexa Fluor 568, followed by filipin staining. A representative image is shown. (*B*) Ac_4ManNAz-labeled control and NPC1-null fibroblasts were incubated with DIBO; costained with monoclonal antibodies to EEA1, CD63, and LAMP1; and then incubated with appropriate secondary antibodies and visualized by confocal microscopy. n = 20–30 cells scored per condition; three independent experiments.

or lysosomal vesicles or the accumulation of this marker within endosomes (28). Nonetheless, these results strongly indicate that the accumulation of SiaNAz-containing glycoconjugates occurs within endosomes and not lysosomes.

Considering that the NPC1-null fibroblasts that we used in this study lack the NPC1 protein, it is also possible that some colocalization with this lysosomal marker could occur in cells with partial loss of NPC1 function. Consistent with this notion, we observed the greatest degree of colocalization between SiaNAz and LAMP1 in NPC2-deficient fibroblasts (Fig. S4), with some additional colocalization found with CD63, but not with EEA1.

Accumulation of Sialylated Molecules Within Endosomes Can Be Attributed Largely to Impaired Recycling. The buildup of sialylated molecules within endosomal compartments could result from impaired recycling of these glycoconjugates back to the cell surface or from the inability of endosomes to fuse with lysosomes, thereby facilitating their turnover. To address mechanisms for the endosomal localization of sialylated cargo, we performed DIBO experiments in combination with the fluorophore-conjugated endocytic uptake marker dextran. Once endocytosed, dextrans are capable of trafficking to lysosomes, where they accumulate owing to lack of efficient degradation. Colocalization of dextran and the labeled glycoconjugates in endosomes would support impaired lysosome/endosome fusion, indicating that neither type of molecule is able to reach the lysosome. In contrast, failure of labeled glycoconjugates to colocalize with lysosomal dextran would support impaired recycling of the glycoconjugates to the cell surface as the most likely mechanism, because the ability of tracer molecules (e.g., dextran) to reach the lysosome would not be impaired in these cells.

Fluorophore-tagged dextran is capable of reaching perinuclear compartments representative of lysosomes or late endosomes in both NPC1-null and NPC2-deficient cells (Fig. 3*A*), arguing against a general defect in endocytic trafficking to these compartments. We found only minimal colocalization of dextran with sialylated glycoconjugates, particularly within vesicles located at the cell periphery (see arrows). This lack of colocalization supports the idea that endosomal accumulation of sialylated molecules in NPC cells likely is due primarily to impaired recycling, and not to the inability of endosomes to fuse with lysosomes. Although closely juxtaposed, we were also unable to detect colocalization of dextran and filipin in these cells (Fig. 3*B*), indicating a surprising level of compartmentalization of endocytosed molecules within NPC cells.

Endocytic Accumulation Involves Mainly Glycoproteins. We next examined the nature of the sialylated glycoconjugates accumulating in NPC1-null cells, using inhibitors of glycosylation. Ac_4ManNAz-labeled NPC1-null and NPC2-deficient fibroblasts were first treated with the *O*-glycan biosynthesis inhibitor benzyl α-GalNAc (GB) or with the *N*-glycan processing inhibitor kifunensine (Kf) and analyzed by confocal microscopy. The ability of Kf to inhibit *N*-glycan processing, and thereby reduce acceptors for sialic acid, in NPC cells was confirmed in independent experiments (Fig. S5). Both compounds effectively reduced the overall SiaNAz staining as well as the intensity and amount of vesicular staining, indicating that primarily endocytosed glycoproteins were labeled.

We next treated Ac_4ManNAz-labeled cells with *N*-butyl-deoxygalactonojirimycin (NB-DGJ), an inhibitor of glycolipid biosynthesis and an approved treatment for NPC disease (29), followed by SPAAC and visualization of glycoconjugates by confocal microscopy (Fig. S6). In parallel, we performed filipin staining to gauge the effects of this compound on cholesterol storage. We used NB-DGJ was used instead of N-butyl-deoxynojirimycin (NB-DNJ) since it has been shown to be a more specific and potent inhibitor of glucosylceramide synthase in cells (30). High performance thin layer chromatography (HP-TLC) analysis

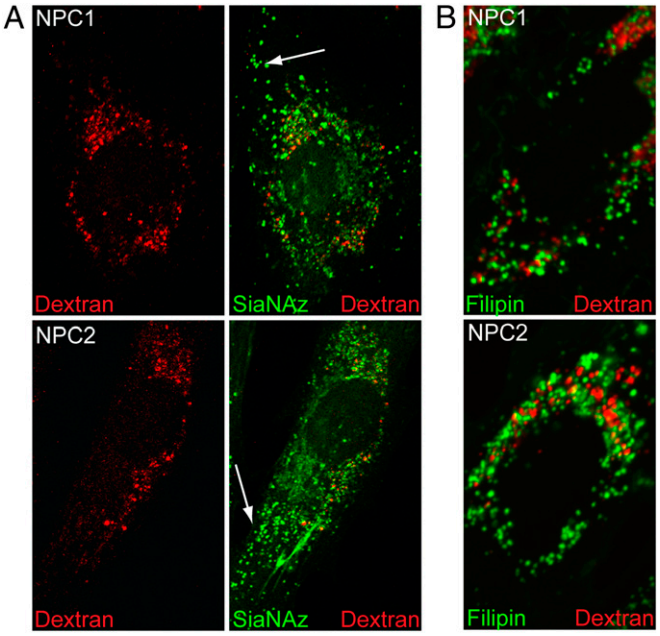

Fig. 3. Accumulation of sialylated molecules within endosomes of NPC cells can be attributed largely to impaired recycling. (*A*) Ac_4ManNAz-labeled NPC1-null and NPC2-deficient fibroblasts were incubated with 0.5 mg/mL Alexa Fluor 647–conjugated dextran for 12 h and then chased for 3 h to allow internalization of this endocytic tracer. Cells were visualized by confocal microscopy. Arrows denote the lack of colocalization between internalized dextran and sialylated molecules within peripheral vesicles. (*B*) Ac_4ManNAz-labeled NPC1-null and NPC2-deficient fibroblasts were incubated with dextran as above and costained with filipin. Cells were visualized by fluorescence microscopy. n = 20–22 cells scored per condition; three separate experiments.

demonstrated an ∼50% reduction in glycolipid levels (Fig. S6). Despite this reduction, no decrease in filipin staining or accumulation of SiaNAz-positive vesicles was detected (Fig. S6). These results are in agreement with a previous study showing variable reduction in glycosphingolipid (GSL) biosynthesis in cultured cells but only minimal changes in cholesterol storage (11).

Methyl β-Cyclodextrin Treatment Corrects Cholesterol Storage and the Intracellular Accumulation of Sialylated Glycoproteins. Another treatment strategy proposed for NPC disease includes alleviation of cholesterol storage by treatment with β-cyclodextrin (8, 31–36). We treated Ac_4ManNAz-labeled NPC1-null and NPC2-deficient fibroblasts with methyl β-cyclodextrin (MβCD) and used confocal microscopy to analyze the impact of MβCD on NPC phenotypes. Treatment of NPC1-null cells with MβCD effectively reduced the accumulation of both cholesterol and sialylated glycoconjugate (Fig. 4*A*). Qualitative assessment of the data revealed only minimal filipin and vesicular SiaNAz staining. Moreover, quantification of three independent experiments showed correction of the SiaNAz phenotype in >90% of cyclodextrin-treated NPC1-null and NPC2-deficient cells (Fig. 4*B*).

Cyclodextrin has been shown to inhibit endocytosis by modulating cholesterol levels within lipid rafts (37). To rule out the possibility that decreased endocytosis of sialylated molecules accounts for the loss of intracellular SiaNAz staining, we labeled control, NPC1-null, and NPC2-deficient fibroblasts with Ac_4ManNAz and peracetylated *N*-acetylmannosamine (Ac_4ManNAc) in the presence or absence of cyclodextrin and measured total surface fluorescence intensity (Fig. 4*C* and Fig. S7). Only slight changes in total cell surface fluorescence intensity were detected in all treated cells, indicating that surface sialylation is not significantly altered by the

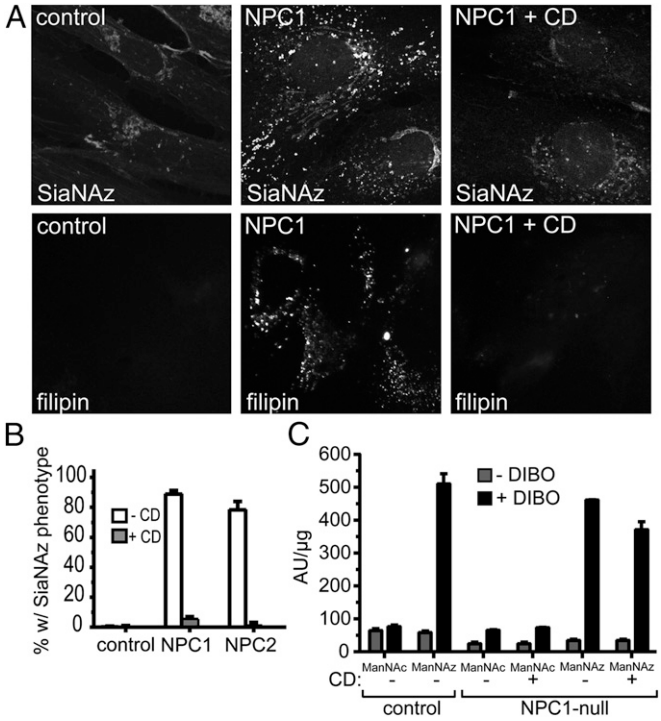

Fig. 4. MβCD treatment of NPC1-null fibroblasts corrects cholesterol storage and the intracellular accumulation of sialylated molecules. (*A*) Cells were labeled with Ac_4ManNAz for 48 h in the presence or absence of MβCD (CD; 300 μM for 24 h), followed by reaction with DIBO and filipin staining and visualization by fluorescence microscopy. $n = 21–24$ cells scored in a blinded fashion per condition; three independent experiments. (*B*) The percentage of cells displaying vesicular SiaNAz staining was quantified in control, NPC1-null, and NPC2-deficient fibroblasts. (*C*) Control and NPC1-null fibroblasts were labeled with Ac_4ManNAz in the presence or absence of MβCD, and surface fluorescence intensity was measured. The results in *B* and *C* represent three independent experiments. Error bars indicate SDs.

presence of MβCD. Thus, it appears that the loss of intracellular SiaNAz in NPC fibroblasts induced by cyclodextrin treatment is related to alleviation of cholesterol storage, which results in the restoration of normal lysosomal turnover of sialoglycoproteins.

Discussion

The results presented here demonstrate that the chemical reporter strategy combined with pharmacologic treatment can provide unprecedented insight into endocytic trafficking defects associated with a human disease. This technology was exploited to uncover a striking build-up of glycoproteins within endosomes of NPC fibroblasts that was completely separate from cholesterol-filled compartments. Chemical induction of cholesterol storage by imipramine led to similar glycoprotein accumulation, indicating that cholesterol storage is primarily responsible for this phenotype. This mechanism is supported by the observation that treatment of NPC cells with cyclodextrin alleviates cholesterol and glycoprotein accumulation. The observed phenotype is specific to NPC cells, with no detectable sialylated glycoconjugate accumulation seen in MPS-I or ML-IV cells.

We have shown that cholesterol storage leads to abundant accumulation of glycoproteins in endosomes, as judged by the profound decreases in SiaNAz staining after treatment of NPC cells with glycoprotein glycosylation inhibitors. In contrast, treatment of NPC fibroblasts with the glycolipid inhibitor NB-DGJ, which led to an ∼50% reduction in total GSL levels, did not affect cholesterol storage or glycoprotein recycling in the NPC fibroblasts. These results are surprising, given the previously reported relationship between cholesterol and ganglioside storage in NPC disease (9, 38). It is possible that the observed level of reduction in glycolipid biosynthesis is not sufficient to alter the cholesterol storage phenotype, in a manner similar to what has been seen in knockout mice lacking GSL biosynthetic enzymes (9, 38). Moreover, fibroblasts synthesize limited types of gangliosides, and thus the complex types found in neural tissue might play a more significant role in the cholesterol storage phenotype (9, 38, 39).

Few examples of endosomal accumulation of glycoproteins have been reported to date (10, 14). Experiments using the endocytic uptake marker dextran showed that impaired recycling, and not endosome/lysosome fusion, is primarily responsible for the endosomal accumulation of sialoglycoproteins—a finding consistent with observations on transferrin receptor recycling in NPC1-deficient CHO cells (10). Considering that many signal transduction events, including ligand–receptor binding and coordination of second messengers, occur within endosomes, we speculate that some of the phenotypes associated with NPC disease may arise from impaired recycling of glycoproteins involved in cell signaling. The decreased residence of these glycoproteins at the cell surface of neurons or other sensitive cell types, their prolonged localization within endosomes, or their failure to turn over efficiently could disrupt the balance of key pathways involved in survival and function of affected tissues. The alleviation of this recycling phenotype after cyclodextrin treatment provides additional support for the idea that cholesterol storage represents the primary driver of endosomal glycoprotein accumulation in NPC cells. If cholesterol and glycoprotein accumulation were independent phenomena, then the loss of filipin staining after cyclodextrin treatment would not be expected to resolve the vesicular SiaNAz staining.

Chemical reporter strategies have been applied to visualize glycans in cells and living organisms with success (18–25), however, insights into the functional relevance of glycans in normal and disease biology have yet to emerge from these applications. Our findings pave the way for the use of chemical reporter strategies to study the impact of altered glycosylation on the pathophysiology of human diseases. We believe that this approach will find value in the diagnosis of certain disorders and in the identification of other diseases involving altered trafficking of endocytosed glycoconjugates. The combined use of metabolic labeling of cells and subsequent functionalization of their glycoconjugates with the isolation and proteomic-based identification of individual glycoproteins with altered trafficking or localization can be expected to uncover previously unrecognized aspects of human disease.

Materials and Methods

Chemicals and Biological Reagents. Imipramine, filipin, and MβCD were obtained from Sigma-Aldrich. Goat anti-rabbit IgG(H+L) Alexa-Fluor 488, goat anti-mouse IgG(H+L) Alexa Fluor 488, and strepavidin Alexa Fluor 568 were obtained from Invitrogen. NB-DGJ was obtained from Toronto Research Chemicals. The monocolonal mouse antibody anti-CD63 (H5C6) and LAMP-1 antibody (H4A3) were obtained from the Developmental Studies Hybridoma Bank, developed under the auspices of the Eunice Kennedy Shriver National Institute of Child Health and Human Development and maintained by the Department of Biology, University of Iowa. Mouse monoclonal antibody to EEA1 was obtained from BD Biosciences. Fluorescent-conjugated dextran (M_r 10,000) was obtained from Molecular Probes. The synthetic compound DIBO was reconstituted in dimethylformamide (DMF) and stored at –80 °C until use. Final concentrations of DMF never exceeded 0.56%, to avoid toxic effects.

Cell Lines and Culture. The NPC1-null cells (a gift from Dr. Daniel Ory, Washington University School of Medicine) were fibroblasts isolated from a patient with no detectable NPC1 protein, and the NPC2-deficient cells were fibroblasts obtained from the National Institute of General Medical Sciences (NIGMS) Human Genetic Cell Repository (GM18455) that were originally isolated from a compound heterozygous NPC patient with nonsense and missense mutations in the NPC2 gene. Allele 1 carries a substitution (G > T) at nucleotide 58 (c.58G > A) in exon 1, resulting in a nonsense mutation at codon 20 [E20× (GLU20TER)]; allele 2 carries a substitution (G > T) at nucleotide 140 (c.140G > T) in exon 2, resulting in a missense mutation at

codon 47. Human skin control fibroblasts (CRL-1509; American Type Culture Collection), NPC1-null fibroblasts, NPC2-deficient fibroblasts, ML-IV fibroblasts (GM02048; NIGMS Human Genetic Cell Repository), and MPS I fibroblasts (GM00798; NIGMS Human Genetic Cell Repository) were cultured in DMEM (American Type Culture Collection) with L-glutamine (2 mM), sodium bicarbonate (1.5 g/L), glucose (4.5 g/L), Hepes (10 mM), and sodium pyruvate (1.0 mM). The medium was further supplemented with penicillin (100 U/mL)/streptomycin (100 μg/mL; Mediatech) and FBS (10% or 20%; BenchMark). Cells were maintained in a humid 5% CO_2 atmosphere at 37 °C and subcultured every 2–3 d.

Metabolic Labeling, Cycloaddition Chemistry, and Staining of Cells. Fibroblast cultures were seeded at a density of 50,000 cells per coverslip (22 mm) and allowed to adhere overnight, and then labeled with Ac_4ManNAz (25 μM) or Ac_4GalNAz (25 μM) for 2 d. Monolayers were incubated with DIBO (30 μM) for 1 h at room temperature, washed three times in PBS, and fixed with formaldehyde (3.7%) for 15 min at room temperature. The cells were then permeabilized for 10 min at room temperature using Triton X-100 (0.2%) in PBS, washed, and incubated with strepavidin Alexa Fluor 568 (1:100) in PBS containing Triton X-100 (0.2%) for 30 min at room temperature. Coverslips were washed three times in PBS and mounted on glass slides for imaging by fluorescence or confocal microscopy.

In some experiments, cells were costained with filipin before imaging. After incubation with streptavidin Alexa Fluor 568, cells were incubated with filipin (0.05 mg/mL) in PBS containing FBS (10%) for 1 h at room temperature in the dark, followed by three washes with PBS. For costaining of Ac_4ManNAz-labeled cells with antisera to protein markers, cells were first incubated with DIBO, then permeabilized for 10 min at room temperature using Triton X-100 (0.2%) in PBS, washed, and incubated with the following specific monoclonal antibodies: mouse anti-EEA1 (early endosomes), mouse anti-CD63 (late endosomes/multivesicular bodies), and mouse anti-LAMP1 (lysosomes) for 1 h. After washing, the slides were incubated with goat anti-mouse Alexa Fluor 488 (to stain the protein markers) and with streptavidin Alexa Fluor 568 (to stain the SiaNAz-containing molecules) and then imaged by confocal microscopy.

For experiments with fluorophore-tagged dextran, NPC1-null and NPC2-deficient cells were incubated with Ac_4ManNAz for 2 d and then pulsed with 0.5 mg/mL dextran-conjugated dye (dextran Alexa Fluor 647; M_r 10,000) in the culture medium for 12 h at 37 °C. The dextran-containing medium was then removed, and the cells were chased in serum-free medium for 3 h to facilitate delivery of contents to lysosomal compartments.

Drug Treatments. NPC1-null and NPC2-deficient fibroblasts were treated with Ac_4ManNAz (25 μM) in the presence of the glucosylceramide synthase inhibitor NB-DGJ (100 μM) for 5 d; imipramine (50 μM), phenelzine (50 μM), GB (2 mM), and Kf (10 μM) for 2 d; or MβCD (300 μM) for 1 d before preparation for imaging as described above. Cells were washed three times, incubated with DIBO (30 μM) for 1 h at room temperature, fixed, permeabilized, and stained with streptavidin Alexa Fluor 568 or, alternatively, washed, fixed, and stained with filipin as described previously. Coverslips were washed three times in PBS for 5 min each wash and mounted on to glass slides. Fluorescent cells were observed by confocal microscopy or fluorescence microscopy using a UV filter set. To quantify the extent of correction in drug-treated NPC1-null cells, 150–200 cells from three independent experiments were assessed for the presence of peripherally localized vesicular SiaNAz staining. The average percentage of corrected cells was recorded.

Surface Azide Labeling and Fluorescence Intensity Measurements. Fibroblast cultures were grown in the presence of Ac_4ManNAz (100 μM final concentration) for 2 d, as before. The cells were either not treated or treated with MβCD (300 μM) for 1 d. WT human skin fibroblast, NPC1-null, and NPC2-deficient cells bearing azides and control cells grown in the presence of Ac_4ManNAc (100 μM final concentration) were incubated with the biotinylated compound DIBO (30 μM) in labeling buffer (PBS, pH 7.4, containing 1% FBS) for 1 h at room temperature. The cells were washed three times with labeling buffer and then incubated with avidin conjugated to FITC (0.5 μg/mL; Molecular Probes) for 15 min at 4 °C. After three washes and cell lysis, cell lysates were analyzed for fluorescence intensity (485 ex/520 em) using a microplate reader (BMG Labtech). Data points were collected in triplicate and are representative of three separate experiments. Cell viability was assessed at different points in the procedure with exclusion of trypan blue.

Fluorescence and Confocal Microscopy. Initial analysis was performed on a Zeiss Axioplan 2 fluorescence microscope. Confocal images were acquired using a 60× (NA1.42) oil objective. Stacks of optical sections were collected in the *z* dimension. The step size, based on the calculated optimum for each objective, was between 0.25 and 0.5 μm. Subsequently, each stack was collapsed into a single image (*z*-projection). Analysis was performed offline using ImageJ 1.39f software and Adobe Photoshop CS3 extended version 10.0, with all images treated equally.

ACKNOWLEDGMENTS. We thank Dr. Daniel Ory (Washington University School of Medicine) for providing the NPC1-null fibroblasts and Dr. Kazuhiro Aoki (University of Georgia) for assisting with the high performance thin layer chromatography analysis of glycolipids. This research was supported by National Center for Research Resources Grant P41RR05351 (to G.-J.B.) and National Institute of General Medical Sciences Grants 8P41GM103390 (to G.-J.B.) and R01 GM086524 (to R.S.) through the National Institutes of Health.

1. Infante RE, et al. (2008) NPC2 facilitates bidirectional transfer of cholesterol between NPC1 and lipid bilayers, a step in cholesterol egress from lysosomes. *Proc Natl Acad Sci USA* 105(40):15287–15292.
2. Wang ML, et al. (2010) Identification of surface residues on Niemann-Pick C2 essential for hydrophobic handoff of cholesterol to NPC1 in lysosomes. *Cell Metab* 12(2): 166–173.
3. Rosenbaum AI, Maxfield FR (2011) Niemann-Pick type C disease: Molecular mechanisms and potential therapeutic approaches. *J Neurochem* 116(5):789–795.
4. Walkley SU, Suzuki K (2004) Consequences of NPC1 and NPC2 loss of function in mammalian neurons. *Biochim Biophys Acta* 1685(1-3):48–62.
5. Paul CA, Boegle AK, Maue RA (2004) Before the loss: Neuronal dysfunction in Niemann-Pick type C disease. *Biochim Biophys Acta* 1685(1-3):63–76.
6. Lloyd-Evans E, et al. (2008) Niemann-Pick disease type C1 is a sphingosine storage disease that causes deregulation of lysosomal calcium. *Nat Med* 14(11):1247–1255.
7. Lloyd-Evans E, Platt FM (2010) Lipids on trial: The search for the offending metabolite in Niemann-Pick type C disease. *Traffic* 11(4):419–428.
8. Madra M, Sturley SL (2010) Niemann-Pick type C pathogenesis and treatment: From statins to sugars. *Clin Lipidol* 5(3):387–395.
9. Gondré-Lewis MC, McGlynn R, Walkley SU (2003) Cholesterol accumulation in NPC1-deficient neurons is ganglioside-dependent. *Curr Biol* 13(15):1324–1329.
10. Pipalia NH, Hao M, Mukherjee S, Maxfield FR (2007) Sterol, protein and lipid trafficking in Chinese hamster ovary cells with Niemann-Pick type C1 defect. *Traffic* 8(2): 130–141.
11. te Vruchte D, et al. (2004) Accumulation of glycosphingolipids in Niemann-Pick C disease disrupts endosomal transport. *J Biol Chem* 279(25):26167–26175.
12. Devlin C, et al. (2010) Improvement in lipid and protein trafficking in Niemann-Pick C1 cells by correction of a secondary enzyme defect. *Traffic* 11(5):601–615.
13. Simons K, Gruenberg J (2000) Jamming the endosomal system: Lipid rafts and lysosomal storage diseases. *Trends Cell Biol* 10(11):459–462.
14. Cabeza C, et al. (2012) Cholinergic abnormalities, endosomal alterations and up-regulation of nerve growth factor signaling in Niemann-Pick type C disease. *Mol Neurodegener* 7(1):11.
15. Martin OC, Pagano RE (1994) Internalization and sorting of a fluorescent analogue of glucosylceramide to the Golgi apparatus of human skin fibroblasts: Utilization of endocytic and nonendocytic transport mechanisms. *J Cell Biol* 125(4):769–781.
16. Ning X, Guo J, Wolfert MA, Boons GJ (2008) Visualizing metabolically labeled glycoconjugates of living cells by copper-free and fast huisgen cycloadditions. *Angew Chem Int Ed Engl* 47(12):2253–2255.
17. Sletten EM, Bertozzi CR (2009) Bioorthogonal chemistry: Fishing for selectivity in a sea of functionality. *Angew Chem Int Ed Engl* 48(38):6974–6998.
18. Boons GJ (2010) Bioorthogonal chemical reporter methodology for visualization, isolation and analysis of glycoconjugates. *Carbohydr Chem* 36:152–167.
19. Prescher JA, Bertozzi CR (2005) Chemistry in living systems. *Nat Chem Biol* 1(1):13–21.
20. Laughlin ST, Bertozzi CR (2007) Metabolic labeling of glycans with azido sugars and subsequent glycan-profiling and visualization via Staudinger ligation. *Nat Protoc* 2(11):2930–2944.
21. Mbua NE, Guo J, Wolfert MA, Steet R, Boons GJ (2011) Strain-promoted alkyne-azide cycloadditions (SPAAC) reveal new features of glycoconjugate biosynthesis. *ChemBioChem* 12(12):1912–1921.
22. Baskin JM, et al. (2007) Copper-free click chemistry for dynamic in vivo imaging. *Proc Natl Acad Sci USA* 104(43):16793–16797.
23. Dehnert KW, et al. (2011) Metabolic labeling of fucosylated glycans in developing zebrafish. *ACS Chem Biol* 6(6):547–552.
24. Laughlin ST, Baskin JM, Amacher SL, Bertozzi CR (2008) In vivo imaging of membrane-associated glycans in developing zebrafish. *Science* 320(5876):664–667.
25. Rabuka D, Hubbard SC, Laughlin ST, Argade SP, Bertozzi CR (2006) A chemical reporter strategy to probe glycoprotein fucosylation. *J Am Chem Soc* 128(37):12078–12079.
26. Friscourt F, et al. (2012) Polar dibenzocyclooctynes for selective labeling of extracellular glycoconjugates of living cells. *J Am Chem Soc* 134(11):5381–5389.
27. Rodriguez-Lafrasse C, et al. (1990) Abnormal cholesterol metabolism in imipramine-treated fibroblast cultures: Similarities with Niemann-Pick type C disease. *Biochim Biophys Acta* 1043(2):123–128.
28. Kobayashi T, et al. (2000) The tetraspanin CD63/lamp3 cycles between endocytic and secretory compartments in human endothelial cells. *Mol Biol Cell* 11(5):1829–1843.

29. Platt FM, Jeyakumar M (2008) Substrate reduction therapy. *Acta Paediatr Suppl* 97(457):88–93.
30. Andersson U, Butters TD, Dwek RA, Platt FM (2000) N-butyldeoxygalactonojirimycin: A more selective inhibitor of glycosphingolipid biosynthesis than N-butyldeoxynojirimycin, in vitro and in vivo. *Biochem Pharmacol* 59(7):821–829.
31. Abi-Mosleh L, Infante RE, Radhakrishnan A, Goldstein JL, Brown MS (2009) Cyclodextrin overcomes deficient lysosome-to-endoplasmic reticulum transport of cholesterol in Niemann-Pick type C cells. *Proc Natl Acad Sci USA* 106(46):19316–19321.
32. Davidson CD, et al. (2009) Chronic cyclodextrin treatment of murine Niemann-Pick C disease ameliorates neuronal cholesterol and glycosphingolipid storage and disease progression. *PLoS ONE* 4(9):e6951.
33. Liu B, et al. (2010) Cyclodextrin overcomes the transport defect in nearly every organ of NPC1 mice leading to excretion of sequestered cholesterol as bile acid. *J Lipid Res* 51(5):933–944.
34. Rosenbaum AI, Zhang G, Warren JD, Maxfield FR (2010) Endocytosis of beta-cyclodextrins is responsible for cholesterol reduction in Niemann-Pick type C mutant cells. *Proc Natl Acad Sci USA* 107(12):5477–5482.
35. Rujoi M, Pipalia NH, Maxfield FR (2010) Cholesterol pathways affected by small molecules that decrease sterol levels in Niemann-Pick type C mutant cells. *PLoS ONE* 5(9):e12788.
36. Vance JE, Peake KB (2011) Function of the Niemann-Pick type C proteins and their bypass by cyclodextrin. *Curr Opin Lipidol* 22(3):204–209.
37. Rodal SK, et al. (1999) Extraction of cholesterol with methyl-beta-cyclodextrin perturbs formation of clathrin-coated endocytic vesicles. *Mol Biol Cell* 10(4):961–974.
38. Zhou S, et al. (2011) Endosomal/lysosomal processing of gangliosides affects neuronal cholesterol sequestration in Niemann-Pick disease type C. *Am J Pathol* 179(2):890–902.
39. McGlynn R, Dobrenis K, Walkley SU (2004) Differential subcellular localization of cholesterol, gangliosides, and glycosaminoglycans in murine models of mucopolysaccharide storage disorders. *J Comp Neurol* 480(4):415–426.